A Cascadic Geometric Filtering Approach to Subdivision

U. Diewald

Dept. of Math., Univ. of Duisburg, Lotharstrasse 63-65, 47048 Duisburg, Germany

S. Morigi [1]

Dept. of Math., Univ. of Bologna, P.zza di Porta S.Donato 5, 40126 Bologna, Italy

M. Rumpf

Dept. of Math., Univ. of Duisburg, Lotharstrasse 63-65, 47048 Duisburg, Germany

Abstract

A new approach to subdivision based on the evolution of surfaces under curvature motion is presented. Such an evolution can be understood as a natural geometric filter process where time corresponds to the filter width. Thus, subdivision can be interpreted as the application of a geometric filter on an initial surface. The concrete scheme is a model of such a filtering based on a successively improved spatial approximation starting with some initial coarse mesh and leading to a smooth limit surface.

In every subdivision step the underlying grid is refined by some regular refinement rule and a linear finite element problem is either solved exactly or, especially on fine grid levels, one confines to a small number of smoothing steps within the corresponding iterative linear solver. The approach closely connects subdivision to surface fairing concerning the geometric smoothing and to cascadic multigrid methods with respect to the actual numerical procedure. The derived method does not distinguish between different valences of nodes nor between different mesh refinement types. Furthermore, the method comes along with a new approach for the theoretical treatment of subdivision.

Key words: Variational Subdivision, Surface Fairing, Curves & Surfaces, Geometric Modeling, Image Processing

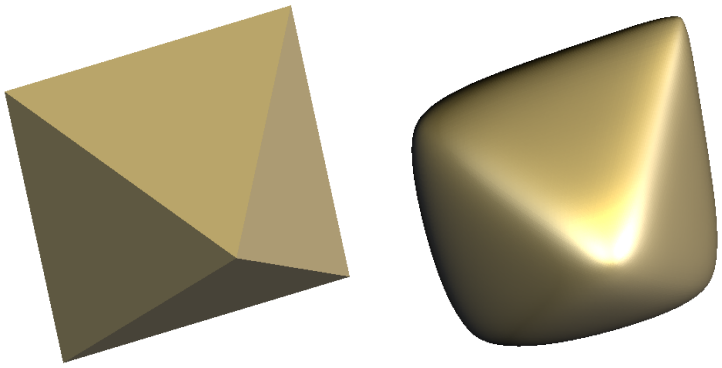

Fig. 1. *Starting from a coarse mesh (left) and considering a spatially varying filter width we obtain a limit surface with locally different smoothness modulus.*

1 Introduction

Multiresolution mesh representation is a key tool used in computer graphics to achieve real-time interaction with large and complex object models. In a multiresolution modeling environment we are able to deal with global shape and structural details of the same object managing meshes of it at different levels of refinement. We then need tools to coarsen a given fine mesh as well as tools for refining a coarse mesh. From fine irregular meshes, produced for example by 3D scanning devices, several approaches have been proposed as mesh simplification, progressive meshes, and surface fairing to obtain a coarser/smoother mesh that forms a surface of arbitrary topology.

Starting from coarse representations of surfaces we can generate appealing smooth representation by iterative applications of refinement steps while keeping the connectivity of the original mesh. Mesh refinement approaches range from multiresolution wavelet-based methods to subdivision schemes, where the quality of the generated mesh is dependent on the subdivision mask used.

We propose a refinement approach that combines the advantages of subdivision (arbitrary topology, local control and efficiency) with those of variational design (high quality surfaces) [30].

The basic idea behind this strategy, first proposed by Kobbelt [19] and named variational subdivision, is to apply, at each subdivision step, a splitting operation to obtain a finer mesh followed by a smoothing operation to update the vertex mesh locations in order to increase the overall smoothness. Kobbelt [21,26] considered energies which involve curvature quantities. The corresponding evolution problems would lead to Willmore flow and surface diffusion respectively, which are fourth order parabolic problems. Whereas we here restrict to second order mean curvature

[1] This work was supported by by MURST, Italy, grant number MM01111258.

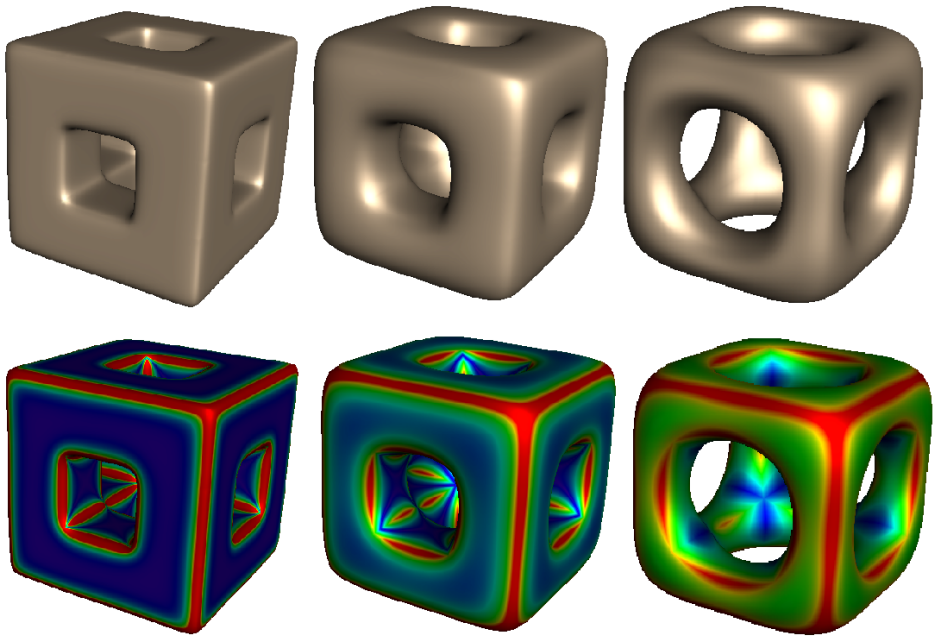

Fig. 2. *Increasing a varying filter width one obtains a scale of subdivision surfaces ranging from smoothed sharp edges up to a smoothing of the complete geometry. On the bottom the corresponding mean curvatures are color coded on the surfaces, especially showing the boundedness of the curvature and giving an indication of bounded second derivatives.*

flow.

In this paper the smoothing step is based on a geometric diffusion and filtering approach related to mean curvature motion, which has already been proved to be very promising for surface fairing purposes [6,7]. Actually, we consider a single fully implicit timestep of mean curvature motion as our smoothing method. In an iteration we successively refine the surface mesh - which turns this approach into a subdivision scheme - and solve a semiimplicit problem to approximate the fully implicit step. This semiimplicit scheme is explicit with respect to the given metric from the last step and implicit concerning the new positions of the nodes. Thus, our method can be regarded as a fixed point iteration, where we simultaneously expect to improve the metric and the resolution. This leads to a suitable geometric smoothing filter on the initial mesh. Our approach is a usual subdivision scheme, but now founded on tools from the theory of geometric evolution problems (mean curvature motion) and numerical linear algebra (cascadic multigrid). We try to outline this new perspective which we believe to offer strong provisions concerning the theoretical analysis of subdivision schemes as well as the range of applications. Furthermore, as already mentioned this approach bridges the gap between subdivision and surface fairing on a rigorous basis. Not very surprisingly, several important questions within this new perspective remain open and require further investigation. Concerning the regularity and convergence we only state conjectures here.

The key aspect for the smoothing step is the geometric diffusion, strictly related

to a well-known physical concept. In physics, in fact, diffusion is known as a process that equilibrates spatial variations in concentration. If we consider some initial concentration function ρ_0 on a domain $\Omega \subset \mathbb{R}^2$ and seek solutions of the linear heat equation $\partial_t \rho - \Delta \rho = 0$ with initial data ρ_0 and natural boundary conditions on $\partial\Omega$, we obtain a scale of successively smoothed concentrations $\{\rho(t)\}_{t\in\mathbb{R}^+}$. For $\Omega = \mathbb{R}^2$ the solution of this parabolic problem coincides with the filtering of the initial data using a Gaussian filter $G_\sigma(x) = (2\pi\sigma^2)^{-1} e^{-x^2/(2\sigma^2)}$ of width or standard deviation σ, i. e. $\rho(\sigma^2/2) = G_\sigma * \rho_0$. In case of surfaces which are graphs we may consider the same process to obtain a smooth representation of an initially coarse graph.

Concerning general surfaces one may ask for analogous evolutionary smoothing strategies. The counterpart of the Euclidean Laplacian Δ on smooth surfaces $\mathcal{M}$ is the Laplace Beltrami operator $\Delta_\mathcal{M}$ and the corresponding evolution applied to the surface coincides with the motion driven by the mean curvature. The aim of this paper is to develope a novel approach to subdivision based on this observation.

Curvature motion is a continuous model, thus we have to discretize it in time and space and to incorporate the iterative process of refinement and subdivision. Concerning the discretization in time it turns out that we can confine to one fully implicit time step of the curvature evolution, like in the heat equation case, where a single implicit time step already has nice smoothing properties. With respect to the spatial discretization we will pick up the cascadic multigrid approach [1] coupled with a suitable fix point iteration in the surface metric.

We obtain a subdivision method which is closely related to standard subdivision schemes concerning the computational complexity. Our approach however has the following advantages:

- Many qualitative properties of the approach can be studied already on the continuous level and do not require a detailed analysis of the discretization.
- The model is independent of the type of meshes, especially of the valences of the mesh nodes, and the considered refinement rules. These characteristics are naturally incorporated in the finite element matrices and do not influence the method's performance significantly (cf. Fig. 6).
- The resulting scheme can easily be adapted to different applications, e. g. to spatially variation of the corresponding filter width (cf. Fig. 1) or to solely smoothing the edges of coarse polygonal models (cf. Fig. 2).

Furthermore, it carries strong provisions for further extensions (cf. Section 9). Finally, we expect the resulting limit surfaces to be $C^{2,\alpha}$-smooth for every $\alpha \in [0, 1)$. By $C^{2,\alpha}$ we denote the Hölder space, i. e. $f \in C^{2,\alpha}$ if f is two times differentiable and all second order partial derivatives are Hölder continuous with respect to the

exponent α, cf. [14].

The paper is organized as follows. In Section 2 we will review subdivision methodology, in Section 3 and 4 the background of geometric diffusion and cascadic numerical methods will be sketched (These sections essentially prepare the terminology and may be skipped by readers already familiar with these topics). Section 5 outlines a simple subdivision scheme for graphs, which already involves the basic features of our approach. Then Section 6 developes the new subdivision approach and Section 7 discusses the algorithmical aspects especially giving details on the involved weights and finite element matrices. An important generalization to non-uniform geometric filter width is given in Section 8. Finally we draw conclusions in Section 9.

Let us emphasize that throughout this paper all surfaces are drawn flat shaded to support a better inspection of the resulting surface smoothness.

2 Review of Subdivision

Classical spline approaches for generating and modeling surfaces, have great difficulties with surfaces of arbitrary topology. On the other hand the variational approach to surface design, where surfaces are computed minimizing some energy functional, can easily deal with arbitrary topology and surface modifications but the computational cost can be very high. Subdivision schemes address the arbitrary topology modeling pretty well, and in addition they come along with results on certain orders of continuity.

Subdivision surface modeling is a lively area of research and a promising approach to the efficient design of surfaces with complex geometry. The basic idea behind subdivision is to refine and smooth a given coarse mesh until a smooth surface is obtained. Suppose our surface is represented as a triangular mesh $\mathcal{M}$ embedded in $\mathbb{R}^3$. Starting with an initial coarse mesh $\mathcal{M}^0$, successive meshes are determined iteratively by the equation

$$\mathcal{M}^k = \mathcal{S}^k(\mathcal{M}^{k-1})$$

where $\mathcal{S}^k$ is the subdivision operator at the k^{th} level which takes the points from level k to points on the finer level $k+1$. Assuming that the subdivision converges, the actual subdivision surface is defined as the limit of this sequence of successive refinements:

$$\mathcal{M} := \lim_{k\to\infty} S^k \circ S^{k-1} \circ \cdots \circ S^1 \mathcal{M}^0.$$

The subdivision schemes for arbitrary topology control meshes come in two classes: approximating and interpolating. Many variants of the approximating schemes have been considered; the classical ones are due to Catmull-Clark [2], and Doo-Sabin [9], who for rectangular meshes considered an extension of quadratic and cubic B-splines, respectively, while a scheme based on quartic box splines on triangular meshes was presented by Loop [23]. An extension of Loop's scheme, introduced by Hoppe et al. [16] incorporates sharp edges on the final limit surface.

Since the ability to control the resulting surface exactly is very important in many applications, a number of interpolating schemes have been proposed to force the limit surface to interpolate particular points [10,11,18,33].

Dyn, Gregory and Levin [10] introduced the butterfly scheme, a simple interpolating subdivision algorithm applicable to arbitrary triangular meshes. Since it only leads to C^1 surfaces in the regular setting (all vertices of the mesh have valence 6), an improved butterfly scheme, the so-called modified butterfly, resulting in smoother surfaces, has been introduced in [33].

All previously mentioned subdivision schemes are based on one of the two tilings of the plane: the tiling with regular triangles and the tiling with squares. However these are not the only refinable tilings: bisection refinement introduced in [29], for example, gives rise to the so called 4-8 subdivision scheme.

For subdivision schemes, the fundamental issue is that about the properties of the limit surface. This includes determining whether a limit object exists and whether that object is smooth.

Most known stationary subdivision schemes generate at least C^1-continuity surfaces on arbitrary meshes in the regular setting [25,31]; while additional criteria based on the eigen structure of the subdivision matrix are required at the extraordinary points to guarantee the smoothness of the limit surface. Recently, the smoothness of the subdivision surfaces in irregular setting (that is near extraordinary vertices) has been rigorously proved in [25,32]. The Loop scheme and the Catmull-Clark schemes, for example, produce surfaces that are C^2-continuous everywhere exept at extraordinary vertices, where they are C^1-continuous. The butterfly scheme is C^1 on regular meshes but not C^1-continuous at extraordinary points, while the modified butterfly scheme guarantees C^1-continuity for arbitrary irregular meshes.

In [19,22] an approach to mesh refinement based on variational methods has been proposed in order to define univariate variational subdivision schemes. Such schemes perform the refinement by uniform subdivision to generate sequences of polygons while the position of the newly inserted vertices is determined by the minimization of a fairness functional measuring a discrete approximation of some bending energy. The well known class of stationary interpolatory refinement schemes is proved to be a special case of these variational schemes. In [20] a similar approach is studied in the bivariate setting of refined triangular meshes.

3 Surface Fairing and Curvature Motion

In this section we will outline evolutionary smoothing methods and their applications in surface fairing. This will motivate our subdivision scheme (cf. Section 7) which generates new triangulated surfaces instead of improving the quality of given surfaces reviewed in this section. Simultaneously we will introduce the basic notation of geometry and geometric differential operators which will be used in the outline and discussion of our subdivision approach. For a detailed introduction to geometry and differential calculus we refer to [8] and [3, Chapter 1]. Let us consider a smooth compact embedded manifold $\mathcal{M} \subset \mathbb{R}^3$ without boundary. Let $x : \Omega \to \mathcal{M} \, ; \, \xi \mapsto x(\xi)$ be some coordinate map from an atlas. For each point x on $\mathcal{M}$ the tangent space $\mathcal{T}_x\mathcal{M}$ is spanned by the basis $\{\frac{\partial x}{\partial \xi_1}, \frac{\partial x}{\partial \xi_2}\}$. By $\mathcal{T}\mathcal{M}$ we denote the tangent bundle. Measuring length on $\mathcal{M}$ requires the definition of a metric $g(\cdot,\cdot) : \mathcal{T}_x\mathcal{M} \times \mathcal{T}_x\mathcal{M} \to \mathbb{R}$. As the corresponding matrix notation we obtain a matrix g whose entries are given by $g_{ij} = \frac{\partial x}{\partial \xi_i} \cdot \frac{\partial x}{\partial \xi_j}$, where $\cdot$ indicates the scalar product in $\mathbb{R}^3$. The entries of the inverse of g are denoted by g^{ij}. The gradient $\nabla_{\mathcal{M}} f$ of a function f is defined as the representation of df with respect to the metric g. In coordinates we obtain

$$\nabla_{\mathcal{M}} f := \sum_{i,j} g^{ij} \frac{\partial (f \circ x)}{\partial \xi_j} \frac{\partial}{\partial \xi_i} \, .$$

We define the divergence $\mathrm{div}_{\mathcal{M}} v$ of a vector field $v \in \mathcal{T}\mathcal{M}$ as the dual operator of the gradient with respect to the L^2-product on $\mathcal{M}$ and obtain in coordinates

$$\mathrm{div}_{\mathcal{M}} v := \sum_i \frac{\partial}{\partial \xi_i} ((v_i \circ x) \sqrt{\det g}) \frac{1}{\sqrt{\det g}} \, .$$

Finally, the Laplace Beltrami operator $\Delta_{\mathcal{M}}$ is given by

$$\Delta_{\mathcal{M}} u := \mathrm{div}_{\mathcal{M}} \nabla_{\mathcal{M}} u \, .$$

With this Laplace Beltrami operator at hand we can define diffusion on surfaces in analogy to the linear diffusion problem in the Euclidean space. Furthermore, we can consider a diffusion of the manifold geometry itself. I. e., we seek a one parameter family of embedded manifolds $\{\mathcal{M}(t)\}_{t \geq 0}$ and corresponding parametrizations $x(t)$, such that

$$\begin{aligned} \partial_t x(t) - \Delta_{\mathcal{M}(t)} x(t) &= 0 \, , \\ \mathcal{M}(0) &= \mathcal{M}_0 \, . \end{aligned}$$

Integration by parts leads to the variational formulation:

$$(\partial_t x, \theta)_{\mathcal{M}(t)} + (\nabla_{\mathcal{M}(t)} x, \nabla_{\mathcal{M}(t)} \theta)_{\mathcal{TM}(t)} = 0$$

for all test functions $\theta \in C^\infty(\mathcal{M}(t))$. Here $(\phi, \psi)_{\mathcal{M}} := \int_{\mathcal{M}} \phi\psi \, \mathrm{d}x$ is the L^2-product on $\mathcal{M}$ and $(v, w)_{\mathcal{M}} := \int_{\mathcal{M}} g(v, w) \, \mathrm{d}x$ is a scalar product on $\mathcal{TM}$, respectively. Already in '91 Dziuk [12] presented a semi implicit finite element scheme for geometric diffusion based on this formulation. The fundamental observation is that this geometric diffusion of the coordinate mapping itself coincides with the motion by mean curvature (MCM) [17]; in fact for any manifold $\mathcal{M}$ we have $\Delta_{\mathcal{M}} x = -H(x)\, N(x)$, and thus we obtain $\partial_t x = -H(x)N(x)$, where $H(x)$ is the corresponding mean curvature (here defined as the sum of the two principal curvatures), and $N(x)$ is the normal on the surface at each point x. For the sake of simplicity we define $MCM(t)\mathcal{M}^0 := \mathcal{M}(t)$, where $\mathcal{M}(t)$ is the solution surface for time t. Thus $MCM(\sigma^2/2)\mathcal{M}$ can be regarded as the application of a "geometric " Gaussian filter of width σ to $\mathcal{M}$. The mean curvature motion model is known as the gradient flow with respect to surface area. This is one indication for the strong regularizing effect of MCM.

Previous work on surface fairing has already involved the concept of curvature motion. On triangulated surfaces as they frequently appear in computer graphics applications, several authors introduced appropriate discretized operators. Taubin [27] and Kobbelt [20] considered an umbrella operator, which is a "spring force type" implementation of the Laplace Beltrami operator. Desbrun et al. [6] considered an implicit discretization of geometric diffusion closely related to Dziuk's approach to obtain strongly stable numerical smoothing schemes.

Finally, to underline the similarities of our discrete, cascadic curvature motion approach to subdivision and the basic finite element implementation of MCM we shortly sketch the numerical algorithm. We have to choose a spatial and a time discretization. Here we follow Dziuk's approach [12]. To clarify the notation we will denote discrete quantities with upper case letters throughout this paper to distinguish them from the corresponding continuous quantities in lower case letters. For the ease of presentation we restrict ourselves to triangular surfaces. We seek a family $\mathcal{M}_h^k$ of discrete successively smoothed surfaces starting from some initial surface $\mathcal{M}_h^0$. Here the subscript h indicates the grid size and k the time step. On surfaces $\mathcal{M}_h$ we define the finite element space of piecewise linear continuous functions V^h. The coordinate vector X can be regarded as a function in $(V^h)^3$. The metric and the gradients of functions on $\mathcal{M}_h$ are evaluated accordingly on each triangle. We expect X^k to be an approximation of $x(k\tau)$ where τ is the selected timestep and discretize the time derivative by a backward Euler scheme as $\partial_t x(k\tau) \approx \tau^{-1}(X^k - X^{k-1})$. Now we are able to formulate our finite element problem making use of the above variational formulation:

Find a family of triangular surfaces $\{\mathcal{M}^k\}_{k\geq 0}$ and corresponding parametrizations

$X^k \in (V^h)^3$, such that

$$(\frac{X^k - X^{k-1}}{\tau}, \Theta)^h_{\mathcal{M}_h^{k-1}} + (\nabla_{\mathcal{M}_h^{k-1}} X^k, \nabla_{\mathcal{M}_h^{k-1}} \Theta)_{\mathcal{T}\mathcal{M}_h^{k-1}} = 0$$

for all discrete test functions $\Theta \in (V^h)^3$. Here, we use the lumped mass scalar product $(\cdot,\cdot)^h_{\mathcal{M}_h}$, which is defined by $(U,V)^h_{\mathcal{M}_h} := \int_{\mathcal{M}_h} \mathcal{I}_h(U\,V)\,\mathrm{d}x$ for two discrete functions $U, W \in V^h$, where $\mathcal{I}_h : C^0(\mathcal{M}_h) \to V^h$ denotes the nodal projection operator (cf. [28]). We can rewrite this using the notation for the discrete Laplace Beltrami operator $(\Delta_{\mathcal{M}_h} U, \Theta)^h_{\mathcal{M}_h} := -(\nabla_{\mathcal{M}_h} U, \nabla_{\mathcal{M}_h}\Theta)_{\mathcal{T}\mathcal{M}_h}$ for all $\Theta \in V^h$. Hence, we obtain

$$\frac{X^k - X^{k-1}}{\tau} - \Delta_{\mathcal{M}_h^{k-1}} X_h^k = 0\,.$$

Finally, in each step of the discrete evolution we have to solve a single system of linear equations. In terms of nodal vectors, which we indicate by a bar on top of the corresponding discrete function we can rewrite the scheme and get

$$(M^{k-1} + \tau L^{k-1})\bar{X}^k = M^{k-1}\bar{X}^{k-1}$$

for the new vertex positions $\bar{X}^k$ at time $t_k = k\,\tau$. Here, we assume the lumped mass matrix M^k and the stiffness matrix L^k, whose entries are given by

$$M^k_{ij} = (\Phi_i, \Phi_j)^h_{\mathcal{M}_h^k}\,,\;\; L^k_{ij} = (\nabla_{\mathcal{M}_h^k}\Phi_i, \nabla_{\mathcal{M}_h^k}\Phi_j)_{\mathcal{T}\mathcal{M}_h^k}\,,$$

to be applied simultaneously to each of the three coordinate components.

4 Cascadic iteration schemes

Multigrid methods [15] are known to be efficient solvers for systems of linear equations $B\,\bar{X} = R$ characterized by an intrinsic hierarchical structure for example resulting from a finite element discretization. Typically an underlying grid hierarchy induces a hierarchical structure on the corresponding discrete function spaces. Let us consider a sequence of finite element spaces $\{V_j\}$, with $V_0 \subset V_1 \subset V_2 \subset \cdots \subset V_j \subset \cdots \subset V_{j_{\max}}$ corresponding to a hierarchy of nested grids $\mathcal{M}_0, \cdots, \mathcal{M}_{j_{\max}}$. In the solution process one typically iterates over j, solving an appropriately restricted system $B_j\bar{X}_j = R_j$ on level j and then refines the grid. Here B_j and R_j are restrictions of $B = B_{j_{\max}}$ and $R = R_{j_{\max}}$, respectively.

Thus, the previously calculated solution $\bar{X}_{j-1}$ can be considered as good initial data for an iterative solver on level j. Somewhat surprising this naive strategy turns out

to be theoretically well founded and robust [1] as long as an error control in the energy norm is considered. Indeed, the number of required iterations or smoothing steps n_j on level j can be fixed a priori. On coarse levels more iterations are required than on finer levels, where very few iterations are sufficient to ensure a required approximation quality on the finest grid level. Even better, Bornemann and Deuflhard [1] proved optimality for this *cascadic* scheme in the sense that the overall cost of the solution process is $O(m)$ where m is the number of unknowns on the finest grid level. Hence under these circumstances one can avoid the more complex nested iterations which a more general multigrid solver would use. In the case of the above surface evolution problems (cf. Section 3), in timestep k we have to solve for $\bar{X} = \bar{X}_k$ given $B = (M^{k-1} + \tau L^{k-1})$ and $R = M^{k-1}\bar{X}^{k-1}$. Here one might apply cascadic iterations as well. But we have to take care of the dependence of the matrices on the metric, which differs with a varying resolution of the mesh. Nevertheless on sufficiently fine grids we expect a negligible impact of this effect on the performance of a cascadic iteration. Obviously, in principle subdivision can be regarded as a cascadic iteration scheme, where one successively applies refinement and smoothing steps. In what follows we will work out this observation in detail.

5 A cascadic linear filtering approach on graphs

At first, let us consider the case of surfaces $\mathcal{M}$, which are graphs in the x_2 direction over a polygonal domain Ω in the x_0, x_1 plane. Here we will outline a very simple but effective subdivision scheme as a first model case, which can actually be interpreted as a variational subdivision scheme. We denote by u the corresponding graph function. Given an initial graph u^0 - which will later be our coarse polygonal mesh - we can ask for a solution u^* of the elliptic partial differential equation

$$(1 - a\,\Delta)u^* = u^0$$

with natural boundary conditions on $\partial\Omega$. This problem corresponds to a single approximate timestep for the heat equation with timestep size $\tau = a$ or the approximation of a Gaussian filter of width $\sqrt{2\tau}$, respectively. For Lipschitz continuous initial data u_0 it is known [13] that the solution is unique and $C^{2,\alpha}$ regular for any $\alpha \in [0, 1)$. Now we approximate u^* by a sequence of linear finite element solutions $\{U^k\}_{k=0,\dots}$ on successively refined regular grids Ω_k for the parameter domain Ω. Due to the convergence properties of linear finite elements [4] we know that for $k \to \infty$ and corresponding vanishing grid size h_k on Ω_k the sequence U^k converges to u^* in the energy as well as in the L^∞ norm. In each step of this procedure we have to solve a linear system of equations of the type

$$(M + a\,L)\bar{U}^k = M\bar{I}_{h_k}u^0$$

where M, L are the mass and stiffness matrix, respectively, and $\bar{I}_{h_k} u^0$ is the linear interpolation of u^0 on Ω_k. The solution U^k minimizes the energy

$$E(U) := \int_{\Omega} (U - u^0)^2 + a\,|\nabla U|^2$$

over all admissible functions U in the k^{th} finite element space. Hence, if u^0 is the function corresponding to a polygonal surface graph over Ω, we can interprete this approach as a variational subdivision approach. As usual the linear systems of equations are solved applying iterative solvers. If we consider a cascadic multigrid method, we can reduce the required number of iterations enormously without effecting the convergence properties (cf. Section 4). Given a final level of resolution $k_{\max}$ we a priori fix the required number of smoothing steps within the cascadic algorithm on all levels following the recipe given by Bornemann and Deuflhard [1]. Then we consider an interpolation of the solution on the previous coarse level as our initial data for the iterative solver on the next level. Finally we end up with a subdivision scheme of optimal complexity. I. e. the cost is proportional to the number of vertices on the finest grid level. Still we know that the resulting sequence of solutions $\{U_{k_{\max}}\}$ convergences to u^*. Thus, our simple iteration leads to $C^{2,\alpha}$ regularity in the limit, independent of the grid type and the applied refinement scheme. Let us briefly summarize the bricks which build up this regularity result for the limit surface. We reference elliptic regularity [13] to check for the regularity of the limit graph, convergence results from basic finite element calculus [4] to prove convergence of the exact finite element solutions to this limit graph, and finally convergence results for the cascadic multigrid to verify that the algebraic error for the multigrid solution of the involved linear systems is of the order of the already controlled finite element error. Hence, applying these well established theories we get nice smoothness properties in this simple case for granted. Unfortunately, most surfaces in computational geometry are not graphs, except from a local perspective. Furthermore, the selection of a parameter domain introduces the metric on that domain as the valid metric for the smoothing process. Thus subdivision results significantly depend on this metric and thereby on the proper choice of the parameter domain. It would be much more natural to apply the same concept based on a single diffusion time step but taking into account the metric on the limit surface or suitable approximations of it, respectively. This will be what we are going to investigate in the following sections.

6 The actual geometric filter process

In Section 3 an 4 we reviewed mean curvature motion and cascadic numerical solvers, respectively. We will now integrate this methodology to derive a new class of subdivision methods. Hence curvature motion and its time discretization will

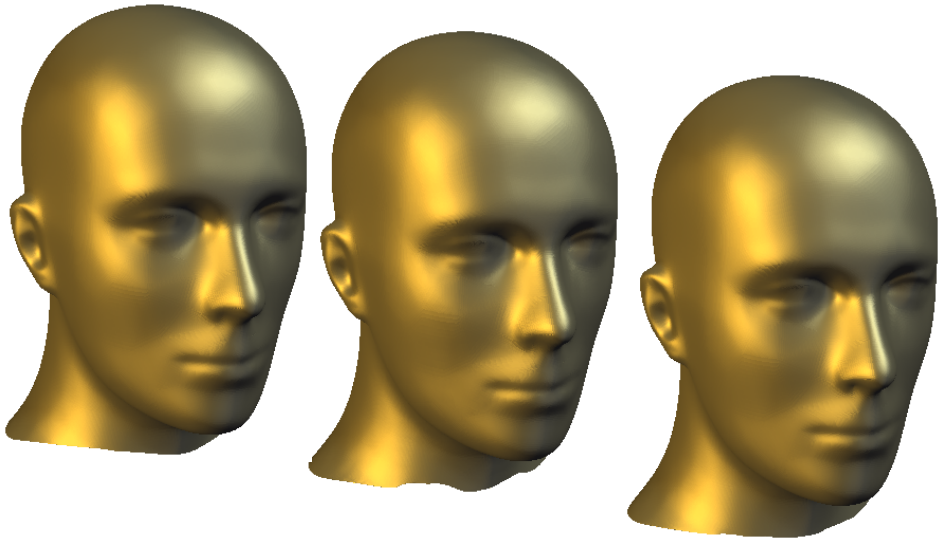

Fig. 3. *Comparison of different subdivision results. From left to right the images correspond to exact solution of the linear systems in each subdivision step, cascadic cg-iterations, and cascadic Jacobi-iterations. Visually there is more or less no difference except close to the boundary in the neck region. This clearly reflects the convergence properties of the cascadic scheme.*

be regarded as appropriate geometric filters and cascadic iterations will serve as suitable solvers. As initial surface we consider any discrete, typically triangulated surface $\mathcal{M}_0$ and denote its parameterization by x_0. To underline the geometric origin and to straighten the presentation we derive our final method in several steps:

Step 1. As it has already been mentioned mean curvature motion is the geometric counterpart of Gaussian filtering and solving the heat equation, respectively. Singularities may arise in MCM of two dimensional surfaces [17], but starting with proper piecewise polygonal surfaces and considering relatively small times t we can assume the evolving surfaces to stay away from the singularities. Then for short times a unique solution exists and it is C^∞-regular. Thus we apply the mean curvature motion semigroup (MCM) as a geometric filter of width σ to $\mathcal{M}_0$ and obtain for a time step $\tau = \frac{\sigma^2}{2}$

$$\mathcal{M} := MCM(\tau)\mathcal{M}_0\,,$$

where the corresponding parametrization is defined by $x := x(\tau)$. A suitable choice for the filter width on a polygonal surface with grid size h_0 appears to be $\sigma \approx h_0$. At first, we assume the triangulation of our initial surfaces to be uniform. In Section 8 we will generalize our method to nonuniform filter width. Alternatively to the correspondence of the filter width and the timestep of MCM, we can incorporate the filter width in the diffusion coefficient and confine to a time step $\tau = 1$. That is, we consider for a spatially fixed filter width σ

$$\partial_t x(t) - a\,\Delta_{\mathcal{M}(t)} x(t) = 0\,,$$

with $a := \frac{\sigma^2}{2}$ and evaluate the evolution at time $t = 1$. As one advantage of this rewriting we can now consider a spatially varying filter width σ (cf. Fig. 1).

Step 2. We can replace the continuous nonlinear semigroup by a time discrete evolution and focus on the first step. In the resulting implicit scheme we have to select a metric (cf. Section 3). We approximate a fully implicit scheme, where the metric is evaluated on the unknown surface, by a sequence of semi implicit schemes. Hence, in each iteration we consider the metric from the previous step and calculate parameterizations x^k of surfaces $\mathcal{M}^k$ for $k > 0$ solving the linear problem

$$(x^k - x_0) - a\,\Delta_{\mathcal{M}^{k-1}} x^k = 0\,.$$

Let us emphasize that the index k does not indicate a curvature motion timestep but only successively improved approximations of the fully implicit scheme

$$(x^* - x_0) - a\Delta_{\mathcal{M}^*} x^* = 0\,.$$

Because of the identity $\Delta_{\mathcal{M}^*} x^* = -H^* N^*$, we have $|H^*| = a\,dist(x^*, x_0)$ where H^* and N^* are the mean curvature and the surface normals of $\mathcal{M}^*$ and $dist(x^*, x_0)$ denotes the one sided distance between $\mathcal{M}^*$ and $\mathcal{M}_0$. Hence, an alternative geometric interpretation of the mean curvature diffusion is that after a timestep a the mean curvature on the resulting surface will be proportional to its distance from the initial surface. Thus, one expects a non-uniform curvature distribution in the final surface, cf. Fig. 10.

For $k \to \infty$ we expect the above iteration to be a fix point iteration with a convergence of the parametrizations x^k at least pointwise to a parametrization x^* of a unique fix point surface $\mathcal{M}^*$. Our numerical results give a strong indication for this convergence. In Section 5 we have already mentioned that a regularity result holds in the simplified case. Given Lipschitz continuous initial data u_0 the solution u^* of $(\mathrm{Id} - a\Delta)u^* = u_0$ is $C^{2,\alpha}$-continuous for any $\alpha \in [0, 1)$ (cf. Sec. 5). Our conjecture is that an analogous regularity result holds for the implicit MCM timestep problem and the Laplace Beltrami operator. Thus, we expect our limit surface to be $C^{2,\alpha}$-continuous for a triangular initial surface (cf. Fig. 6). Experimentally we have verified at least bounded discrete second derivatives (cf. Fig. 2). Rigorous proofs for both the convergence and the smoothness of the limit surface are still missing. We abbreviate the notation and write

$$\mathcal{M}^k = \mathcal{S}(\mathcal{M}^{k-1})\mathcal{M}_0$$

where the argument of the time step operator $\mathcal{S}(\cdot)$ indicates the corresponding metric. The limit surfaces $\mathcal{M}^*$ turns out to be a fix point of the mapping $\mathcal{S}(\cdot)\mathcal{M}_0$,

i. e. $\mathcal{M}^* = \mathcal{S}(\mathcal{M}^*)\mathcal{M}_0$. So far we have derived a geometrically natural smoothing method, which results in solving a sequence of spatially continuous and linear problems.

Step 3. Now we discretize in space, considering triangular surfaces $\mathcal{M}_0$ of different grid size h and corresponding linear finite element spaces V^h and ask for parametrizations $X \in (V^h)^3$ of surfaces $\mathcal{M}_h$ (cf. Section 3). Thus, we consider

$$\mathcal{M}_h^k = \mathcal{S}_h(\mathcal{M}_h^{k-1})\mathcal{M}_0$$

where $\mathcal{S}_h(\cdot)$ denotes the corresponding spatially discrete time step operator. I. e. for the parameterization X^k of $\mathcal{M}_h^k$ we get

$$(X^k - \mathcal{I}_h x_0) - a\,\Delta_{\mathcal{M}_h^{k-1}} X^k = 0\,.$$

Here $\mathcal{I}_h$ again indicates the nodal projection onto V^h. We expect $\mathcal{M}_h^k$ to converge to $\mathcal{M}^*$ for $h \to 0$ (cf. the convergence result by Deckelnick and Dziuk [5]).

Step 4. Furthermore, we consider sequences of nested grids generated by any recursive and regular refinement rule and apply a diagonalization argument with respect to the grid level and the above iteration. After each iteration we refine the grid once and obtain the following subdivision scheme:

$$\mathcal{M}_{h_k}^k = \mathcal{S}_{h_k}(\mathcal{M}_{h_{k-1}}^{k-1})\mathcal{M}_0\,. \tag{1}$$

This corresponds to the operator equation

$$(X_{h_k}^k - \mathcal{I}_{h_k} x_0) - a\,\Delta_{\mathcal{M}_{h_{k-1}}^{k-1}} X_{h_k}^k = 0$$

for the parameterizations $X_{h_k}^k$ of $\mathcal{M}_{h_k}^k$. For the sake of simplicity we write X_k^k, $\mathcal{S}_k$, and $\mathcal{M}_k^k$ instead of $x_{h_k}^k$, $\mathcal{S}_{h_k}$, and $\mathcal{M}_{h_k}^k$, respectively. We suppose geometric decay of the sequence of grid sizes h_k, i. e. $\beta^- h_k \le h_{k+1} \le \beta^+ h_k$. In case of a standard butterfly like refinement rule without smoothing, which results in the splitting of each triangle into four up to scaling identical children, we obtain $\beta^+ = \beta^- = \frac{1}{2}$.

Step 5. In each step of the above subdivision scheme the solution of a system of linear equations (cf. Section 3) is required. As usual in finite element calculus this system is sparse and iterative solvers can be applied. In each subdivision step we modify the metric and refine the underlying grid. This obviously is a cascadic strategy (cf. Section 4) and we know that for increasing iteration indices a decreasing number of smoothing steps n_k in the linear solver has to be performed if we consider appropriately prolongated solutions from the previous level as initial data. Let

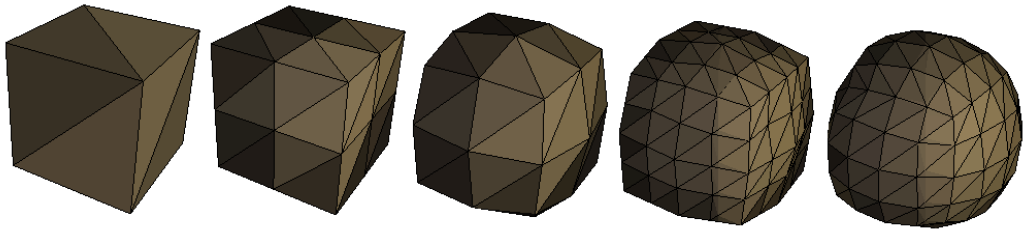

Fig. 4. *A triangulated cube is undergoing two steps of "refine and smooth" following the proposed subdivision scheme.*

us indicate the number of smoothing steps n_k on grid level k by an upper index. Bornemann and Deuflhard proved that the required number of iterations decays geometrically, i. e. in case of conjugate gradient iterations (CG) $n_k = n_{k_{\max}} 2^{\frac{3}{2}(k_{\max}-k)}$ and for the damped Jacobi iteration $n_k = n_{k_{\max}} 2^{2(k_{\max}-k)}$. Given an error tolerance for the algebraic error we can preset the required number of smoothing steps $n_{k_{\max}}$ on the finest grid level $k_{\max}$. In our application we always set $n_{k_{\max}} = 1$. Thus given a final level of refinement $k_{\max}$ up to which we want to iterate the overall cost of the resulting algorithm has optimal complexity for CG in case of a quartering type refinement and nearly optimal complexity for the damped Jacobi iterations. Optimal here means the cost is proportional to the number of fine grid nodes. If the goal is only to ensure appropriate smoothing results, based on our experience one can further reduce the number of iterations n_k especially on fine grid levels k and confine to a fixed number of iterations n. Thus we obtain a suitable approximation of our original model by the iteration

$$\mathcal{M}_k^k = \mathcal{S}_k^{n_k}(\mathcal{M}_{k-1}^{k-1})\mathcal{M}_0\,.$$

Here $\mathcal{S}_k^{n_k}$ represents any iterative solver restricted to n_k iterations in our original subdivision scheme (1) above. Fig. 4 shows a sketch of the general procedure for a very simple example (cf. Fig. 3 and Fig. 5).

As initial data and for the evaluation of the metric we consider the coordinate vector of $\mathcal{M}_{k-1}^{k-1}$ prolongated to level k by trivial interpolation. Let us remark that the number of considered smoothing steps will correspond to the stencil width of our scheme measured in cells (cf. Sec. 7).

To be more precise about the linear finite element problems to be solved in the iteration let us first reformulate the implicit definition of the sequence $\{\mathcal{M}_k^k\}_k$. In discrete variational form we obtain the following problem:

Find a sequence of discrete coordinate maps $\{X_k^k\}_{k=0,\dots}$ with $X_k^k \in (V^{h_k})^3$, which defines a family of triangular surfaces $\{\mathcal{M}_k^k\}_{k=0,\dots}$ such that

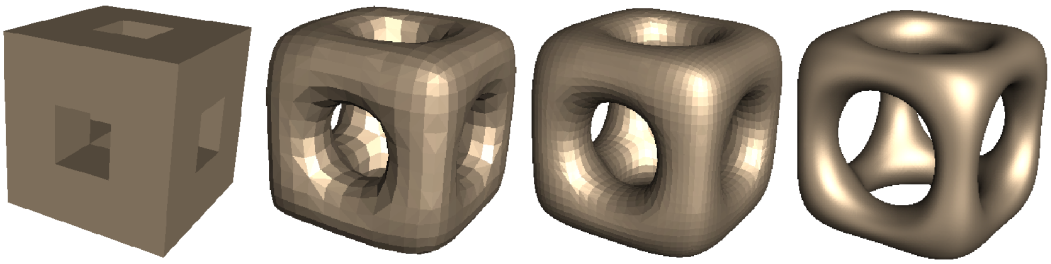

Fig. 5. *A sequence of flat shaded subdivision surfaces subdividing each triangle into four children in each refinement step.*

$$(X_k^k - X_0^k, \Theta)^h_{\mathcal{M}_{k-1}^{k-1}} + (a\nabla_{\mathcal{M}_{k-1}^{k-1}} X_k^k, \nabla_{\mathcal{M}_{k-1}^{k-1}} \Theta)_{\mathcal{T}\mathcal{M}_{k-1}^{k-1}} = 0$$

for all discrete test functions $\Theta \in (V^{h_k})^3$.

Hence, in each iteration step we have to solve the linear system

$$(M^{k-1} + L^{k-1})\bar{X}_k^k = M^{k-1}\bar{X}_0^k\,, \tag{2}$$

where $\bar{X}_k^k$ denotes the nodal vector corresponding to the coordinate function X_k^k and $\bar{X}_0^k$ is the nodal vector corresponding to the trivial interpolation of nodes during the recursive refinement of the initial surface $\mathcal{M}_0$ on grid level k. For the sake of completeness we give precise definitions of the involved lumped mass matrix

$$M_{ij}^{k-1} = (\Phi_i^k, \Phi_j^k)^h_{\mathcal{M}_{k-1}^{k-1}}$$

and the stiffness matrix

$$L_{ij}^{k-1} = (a\nabla_{\mathcal{M}_{k-1}^{k-1}} \Phi_i^k, \nabla_{\mathcal{M}_{k-1}^{k-1}} \Phi_j^k)_{\mathcal{T}\mathcal{M}_{k-1}^{k-1}}$$

which are again simultaneously applied to each of the three coordinate components. These definitions implicitly involve a straightforward prolongation from grid level $k-1$ on which the corresponding metric is given to grid level k on which the basis functions are defined. Here $\{\Phi_i^k\}_i$ denotes the nodal basis of the linear finite element space V^{h_k} on $\mathcal{M}_k^k$.

7 Algorithmical aspects

In the preceding sections we have introduced evolutionary subdivision schemes in a rather abstract frame. Now we will discuss concrete implementation issues.

Let us give some details on the non exact solution of the linear system in each step of our subdivision scheme at least in case of damped Jacobi iterations. In fact,

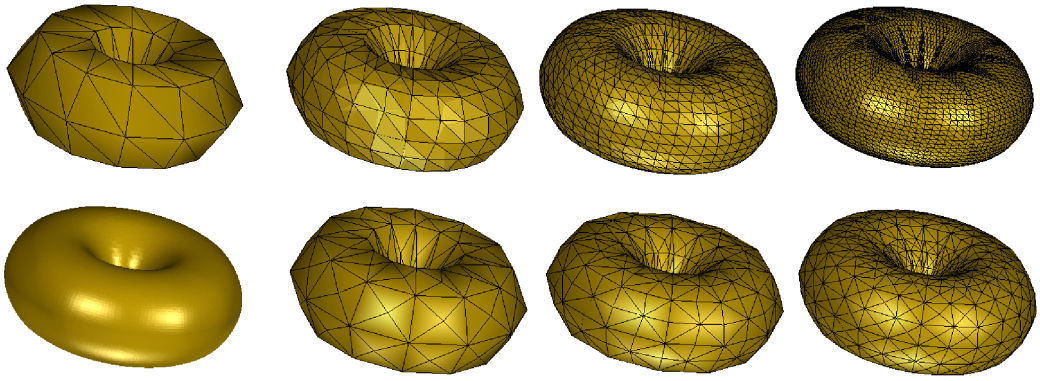

Fig. 6. *A coarse torus (top left) is processed by our subdivision method leading to a smooth limit surface (bottom left). We have used a quartering scheme (top) and a bisection refinement strategy (bottom).*

we confine to a few smoothing steps. We define $\bar{X}^s := S^{n_k}(\bar{X})$ where S is a suitable smoothing operator defined on coordinate vectors, and the exponent n_k indicates the number of considered smoothing steps, i. e. $S^{n+1}(\bar{X}) := S \circ S^n(\bar{X})$. The damped Jacobi iteration S_J is defined by

$$S_J\bar{X} := \bar{X} - \theta\, D^{-1}(M^{k-1}(\bar{X} - \bar{X}_0^k) + L^{k-1}\bar{X})$$

where D is the matrix representing the diagonal part of $(M^{k-1} + L^{k-1})$ and θ is the damping factor. We always have set $\theta = \frac{3}{4}$.

So far we have not specified the refinement method to be applied in every iteration of the presented subdivision schemes. As long as a regular refinement rule is considered which guarantees suitable upper and lower bounds for the angles of the generated triangles our approach in principle is independent of the concrete scheme. Figure 6 depicts two frequently used refinement schemes, the quartering scheme and the recursive bisection scheme. Let us now consider the computation of the involved matrices. The assembly of each matrix M^{k-1}, L^{k-1} - here denoted by B - is based on the standard Finite Element procedure. It consists of an initialization $B = 0$ followed by a traversal of all surface triangles T. On each T with nodes P^0, P^1, P^2, a corresponding local matrix b_{ij}^T is computed first. It corresponds to all pairings of local nodal basis functions. Then the matrix entries are added to the matching entries in the global matrix B, i. e. for every pair i, j we update $B_{\alpha(i),\alpha(j)} = B_{\alpha(i),\alpha(j)} + b_{ij}^T$. Here $\alpha(i)$ is defined as the global index of the node with local index i. Thus we can concentrate on the computation of the local mass matrix m^T and the local stiffness matrix l^T, respectively. Due to the applied lumped mass integration we immediately verify $m_{ij}^T = \frac{1}{3}\delta_{ij}|T|$ where $|T|$ is the area of the triangle T and δ_{ij} the usual Kronecker symbol. For the local stiffness matrix we obtain

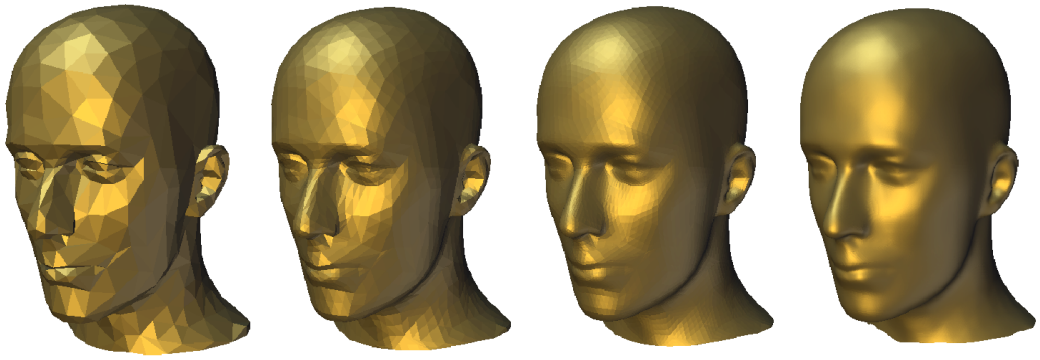

Fig. 7. *A sequence of flatshaded subdivision surfaces is generated using the local filter width algorithm. The starting surface comes along with a very irregular triangular grid (different valences of the nodes, thin triangles, nonhomogeneous grid size), which we keep without changes. The proposed method is able to effectively deal with such surfaces.*

$$l_{ij}^T = a \int_T \nabla_T \phi_i \cdot \nabla_T \phi_j = a\,|T| \frac{\nu_i}{h_i} \cdot \frac{\nu_j}{h_j}$$
$$= a\,|T| \frac{e_i}{h_i\,\|e_i\|} \cdot \frac{e_j}{h_j\,\|e_j\|} = a\,\frac{e_i \cdot e_j}{4|T|}$$

where ϕ_i denotes the nodal base function corresponding to the node x_i for any local index i, ∇_T the gradient on T, and ν_i the outer normal to the edge e_i opposite of x_i. Finally h_i is the height of the triangle over the edge e_i. By construction, these weights coincide with those derived by Pinkall and Polthier, cf. [24].

Let us emphasize that l_{ij} is scale invariant on 2D simplices. After the assembly we obtain the global mass matrix M^{k-1} given by M_{IJ}^{k-1} and the stiffness matrix L^{k-1} given by L_{IJ}^{k-1}. Here uppercase indices are considered as global indices. We immediately get $M_{IJ}^{k-1} = M_I \delta_{IJ}$ where $M_I^{k-1} = \sum_{T, X_I \text{ node of } T} \frac{|T|}{3}$. In case of an m-valence node L^{k-1} has $m+1$ non vanishing entries, which correspond to the node x^I itself and all nodes $x_{\beta(I,j)}$ which are connected to x^I by an edge r_j^I (cf. Fig. 8). Here $\beta(I,j)$ for $j = 1, \cdots, m$ are the global indices corresponding to local indices j of points cyclically ordered around x^I.

Let us denote by T_j^I the triangle spanned by r_j^I and r_{j+1}^I and suppose e_j^I to be the edge of T_j^I opposite to x^I. Then we get

$$L_{I,\beta(I,j)}^{k-1} = a \left(\frac{e_j^I \cdot r_{j+1}^I}{4|T_j^I|} - \frac{e_{j-1}^I \cdot r_{j-1}^I}{4|T_{j-1}^I|} \right),$$
$$L_{II}^{k-1} = a \sum_{1 \le j \le m} \frac{\|e_j^I\|^2}{4|T_j^I|}.$$

Now we have collected all required building blocks of our subdivision scheme. The matrix coefficients turn out to be based on simple geometric calculations. Thus, we

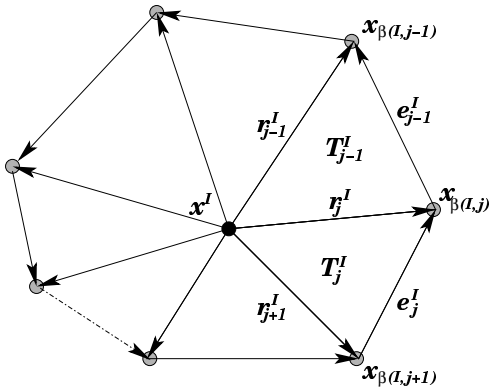

Fig. 8. *A sketch of the local mesh configuration around* x^I.

can write our subdivision scheme in pseudo code notation as follows:

Define $\mathcal{M} := \mathcal{M}^0$ as the initial mesh; $k = 0$;
do {
  $k := k + 1$;
  $\mathcal{M} :=$ *Refinement*$(\mathcal{M})$;
  Compute $M :=$ *MassMatrix*$(\mathcal{M})$
  and $L :=$ *StiffnessMatrix*$(\mathcal{M})$;
  $\bar{X} :=$ nodal vector of $\mathcal{M}$;
  $\bar{X}^0 := \mathcal{I}_{\mathcal{M}} \mathcal{M}^0$;
  for $(n = 0; n < n_k; n = n + 1)$ {
    $\bar{X} := S(\bar{X}^0, M, L)\, \bar{X}$;
  }
  $\mathcal{M} :=$ surface $\mathcal{M}$ with updated nodes $\bar{X}$;
} while ($k \leq k_{\max}$);

Here the operator *Refinement(·)* denotes any regular refinement scheme, whereas *MassMatrix(·)* and *StiffnessMatrix(·)* compute the corresponding matrices on a given surface and $\mathcal{I}_{\mathcal{M}}$ represents the trivial interpolation of the nodal positions of $\mathcal{M}^0$ on $\mathcal{M}$. By trivial interpolation we mean the build in recursive interpolation due to the applied refinement rules without any smoothing operations. Furthermore, $S(\bar{X}^0, M, L)$ is a single smoothing step of an iterative solver for the linear system (2), e. g.

$$S(\bar{X}^0, M, L) = S_J\,.$$

Finally we have to discuss the stencils of dependency during our subdivision iteration. Hence, we call the set of nodes which are connected by at most j edges with a node x the j-neighborhood of x. Multiplying the stiffness matrix L^{k-1} with the vector consisting of the coordinates of the nodes, we obtain a new vector, where each coordinate entry depends on the corresponding old coordinate entry and the coordi-

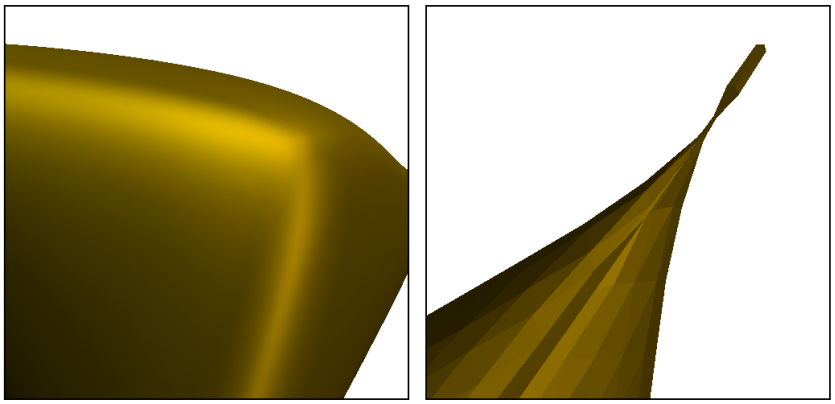

Fig. 9. *The results of the subdivision algorithm applied to a valence* 3 *node. The base triangle formed by the adjacent nodes has uniform edge length* l*, whereas the height of the valence* 3 *node over this triangle is* $\frac{1}{2}\sqrt{2/3}\,l$ *(on the left) and* $2\sqrt{2/3}\,l$ *(on the right). On the left a significant higher refinement level is depicted than on the right due to limitations caused by the instability for sharp corners at the valence* 3 *node on the right.*

nate entries of a 1-neighbourhood of the specific vertex, due to the above explained sparsity pattern of L^{k-1}. Hence, we straightforwardly verify that in each iteration of our subdivision scheme with n_k involved smoothing steps the new position of a node depends on the coordinates of nodes in its n_k-neighborhood.

We tested the method with respect to stability. Thus, we considered the crutial case of a valence 3 node. We found that the method succeeds if the valence 3 node does not form a too sharp corner. However, if the tetrahedron spanned by the node and its adjacent nodes is very thin, numerical instabilities may develop during the evolution process leading to local degeneration of the triangulation, cf. Figure 9.

8 A local filter width expansion

In many applications the initially coarse mesh will be characterized by considerable variations in the local grid size. We can take care of this by adaptation of the filter width in our implicit time step scheme to the local grid size (cf. Fig. 7). Here the idea is to consider a smoothed local grid size of the initial grid as a local filter width and modify the diffusion coefficient with respect to this filter width. Let us emphasize that this grid size function enters our model solely as a filter width. Hence close correspondence to the local edge length is not required. Figure 10 shows a comparison between the expanded model incorporating a smooth local filter width function and the fixed filter width problem studied so far.

In our iterative scheme we apply the same smoothing operators in every step to this local filter width function to ensure still $C^{2,\alpha}$-smoothness of the limit surface.

Hence, we consider the following continuous problem:

$$(x^k - x_0) - \mathrm{div}_{\mathcal{M}^{k-1}} \left(a^{k-1} \nabla_{\mathcal{M}^{k-1}} x^k \right) = 0$$
$$(h^k - h_0) - \mathrm{div}_{\mathcal{M}^{k-1}} \left(a^{k-1} \nabla_{\mathcal{M}^{k-1}} h^k \right) = 0 \,.$$

where $a^k := C^2 \frac{(h^k)^2}{2}$ and h^0 is the initial grid size function. We expect the sequence $\{x^k, h^k\}_k$ to converge to a solution x^*, h^* of the fully implicit problem:

$$(x^* - x_0) - \mathrm{div}_{\mathcal{M}^*} \left(a^* \nabla_{\mathcal{M}^*} x^* \right) = 0$$
$$(h^* - h_0) - \mathrm{div}_{\mathcal{M}^*} \left(a^* \nabla_{\mathcal{M}^*} h^* \right) = 0 \,.$$

where $a^* := C^2 \frac{(h^*)^2}{2}$ and $\mathcal{M}^*$ is the resulting mesh with parameterization x^*. Furthermore, we expect the same regularity result as in the case of fixed filter width, i. e. $C^{2,\alpha}$-smoothness of the limit surface $\mathcal{M}^*$ and of the smoothed filter width function h^*.

We discretize this expanded model following the above guidelines and obtain the following scheme:

Find a sequence of discrete coordinate maps $\{X_k^k\}_{k=0,\dots}$ *with* $X_k^k \in (V^{h_k})^3$ *and discrete functions* $\{H_k^k\}_{k=0,\dots}$ *with* $H_k^k \in V^{h_k}$*, which defines a family of triangular surfaces* $\{\mathcal{M}_k^k\}_{k=0,\dots}$ *such that*

$$(X_k^k - X_k^0, \Theta)^h_{\mathcal{M}_{k-1}^{k-1}} + (A^{k-1} \nabla_{M_{k-1}^{k-1}} X_k^k, \nabla_{M_{k-1}^{k-1}} \Theta)_{\mathcal{T}\mathcal{M}_{k-1}^{k-1}} = 0$$
$$(H_k^k - H_k^0, \Psi)^h_{\mathcal{M}_{k-1}^{k-1}} + (A^{k-1} \nabla_{M_{k-1}^{k-1}} H_k^k, \nabla_{M_{k-1}^{k-1}} \Psi)_{\mathcal{T}\mathcal{M}_{k-1}^{k-1}} = 0$$

for all discrete test functions $\Theta \in (V^{h_k})^3$ *and* $\Psi \in V^{h_k}$.

Here we define $A^k := C^2 \frac{(H_k^k)^2}{2}$ and take $H_k^0 \in V^0$ as the nodal interpolation of the grid size on $\mathcal{M}^0$, that is we define the local filter width function $H(x)$ for any node x on $\mathcal{M}^0$ as the average edge length of all edges form x to adjacent nodes. Thus in each step of our subdivision method we solve the same type of elliptic finite element problem for the coordinate and the filter width function. Besides the additional smoothing of the filter width function the only change concerning the implementation is in the stiffness matrix, which now contains the local weight A^{k-1} instead of the global weight a.

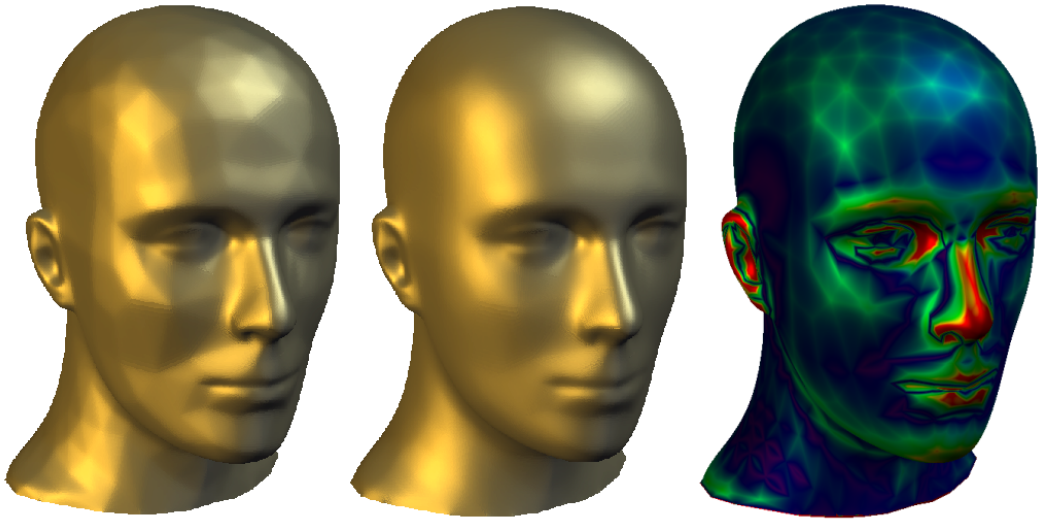

Fig. 10. *A comparison of limit surfaces based on a small and spatially fixed filter width (left) and the local filter width expansion (middle) for a coarse initial grid with considerable variation in the grid size. On the right the color coded modulus of the mean curvature of the surface shown in the middle is depicted.*

9 Conclusions

We have reviewed subdivision methods on the background of surface evolution problems. Thereby, successive smoothing of the discrete surface under consideration is linked to the probably most natural smoothing process on continuous surfaces, which is the motion by mean curvature. The presented method has been embedded in the framework of continuous surface evolution, and corresponding time/space discrete models, respectively. The simultaneous refinement in between the smoothing steps can be performed by any type of regular mesh refinement rule. Furthermore, incomplete linear solvers in the fully discrete schemes lead to the structure of typical subdivision methods. This classifies the methods in terms of finite element calculus as an incomplete cascadic iteration approach in curvature motion. Our interpretation closely relates subdivision methodology and surface fairing. Future work may focus on

- closing the theoretical convergence and smoothness gap,
- comparing the new method with other recent subdivision approaches,
- incorporating anisotropic diffusion and considering additional forcing terms on the right hand side to enable a flexible fine level surface modeling,
- respecting interpolation constraints such as line constraints or average constraints in order to e. g. prescribe sharp edges on the limit surface or to preserve the volume enclosed by the surface during the subdivision process (Let us emphasize that point constraints are not allowed in our setting of a second order evolution problem),
- considering adaptive meshes and corresponding adaptive smoothness control to

reduce the mesh complexity significantly,

- replacing the current setting of a 2^{nd} order diffusion model by some 4^{th} order diffusion, either surface diffusion or Willmore flow.

As we used an experimental code for computing the numerical examples in this paper, we do not include any performance measurements for the proposed subdivision methods and confine to a discussion of the method's complexity.

Acknowledgement

The authors thank Leif Kobbelt and the anonymous referees for valuable comments.

References

[1] F. A. Bornemann and P. Deuflhard. The cascadic multigrid method for elliptic problems. *Numer. Math.*, 75(2):135–152, 1996.

[2] E. Catmull and J. Clark. Recursively generated b-spline surfaces on arbitrary topological meshes. *Computer Aided Design*, 10:350–355, 1978.

[3] I. Chavel. *Eigenvalues in Riemannian Geometry*. Academic Press, 1984.

[4] P. Ciarlet and J. Lions. *Handbook of numerical analysis. Vol. V: Techniques of scientific computing.* Elsevier, 1997.

[5] K. Deckelnick and G. Dziuk. Discrete anisotropic curvature flow of graphs. *Mathematical Modelling and Numerical Analysis*, 33(6):1203–1222, 1999.

[6] M. Desbrun, M. Meyer, P. Schroeder, and A. Barr. Implicit fairing of irregular meshes using diffusion and curvature flow. In *Computer Graphics (SIGGRAPH '99 Proceedings)*, pages 317–324, 1999.

[7] U. Diewald, U. Clarenz, and M. Rumpf. Nonlinear anisotropic diffusion in surface processing. In *Proceedings of IEEE Visualization 2000*, 2000.

[8] M. P. do Carmo. *Riemannian Geometry*. Birkhäuser, Boston–Basel–Berlin, 1993.

[9] D. Doo and M. Sabin. Analysis of the behaviour of recursive division surfaces near extraordinary points. *CAD*, 10(4):356–360, 1978.

[10] N. Dyn, D. Levin, and J. Gregory. A 4-point interpolatory subdivision scheme for curve design. *CAGD*, 4:257–268, 1987.

[11] N. Dyn, D. Levin, and J. Gregory. A butterfly subdivision scheme for surface interpolation with tension control. *ACM Trans. on Graphics*, 9:160–169, 1990.

[12] G. Dziuk. An algorithm for evolutionary surfaces. *Numer. Math.*, 58:603–611, 1991.

[13] M. Giaquinta. *Introduction to regularity theory for nonlinear elliptic systems.* Birkhäuser Verlag, Basel, 1993.

[14] D. Gilbarg and N. S. Trudinger. *Elliptic partial differential equations of second order*. Springer, Berlin, 1983.

[15] W. Hackbusch. *Multi-grid methods and applications.* Springer, Berlin/Heidelberg, 1985.

[16] H. Hoppe, T. DeRose, T. Duchamp, M. Halstead, H. Jin, J. McDonald, J. Schweitzer, and W. Stuetzle. Piecewise smooth surface reconstruction. In *Computer Graphics (SIGGRAPH 1994 Proceedings)*, pages 295–302, 1994.

[17] G. Huisken. The volume preserving mean curvature flow. *J. Reine Angew. Math.*, 382:35–48, 1987.

[18] L. Kobbelt. Interpolatory subdivision on open quadrilateral nets with arbitrary topology. In *Proceedings of Eurographics 96, Computer Graphics Forum*, pages 409–420, 1996.

[19] L. Kobbelt. A variational approach to subdivision. *CAGD*, 13:743–761, 1996.

[20] L. Kobbelt. Discrete fairing. In *Proceedings of the 7th IMA Conference on the Mathematics of Surfaces*, pages 101–131, 1997.

[21] L. Kobbelt. Discrete fairing and variational subdivision for free-form surface design. *The Visual Computer*, 16(3/4):142–158, 2000.

[22] L. Kobbelt and P. Schröder. A multiresolution framework for variational subdivision. *ACM Transactions on Graphics*, 17(4):209–237, October 1998.

[23] C. Loop. Smooth subdivision surfaces based on triangles. *Master Thesis, University of Utah*, 1987.

[24] U. Pinkall and K. Polthier. Computing discrete minimal surfaces and their conjugates. *Exp. Math. 2*, No. 1:15–36, 1993.

[25] U. Reif. A unified approach to subdivision algorithms near extraordinary points. *CAGD*, 12:153–174, 1995.

[26] R. Schneider and L. Kobbelt. Geometric fairing of irregular meshes for free-form surface design. *Computer Aided Geometric Design*, 18:359–379, 2001.

[27] G. Taubin. A signal processing approach to fair surface design. In *Computer Graphics (SIGGRAPH '95 Proceedings)*, pages 351–358, 1995.

[28] V. Thomée. *Galerkin - Finite Element Methods for Parabolic Problems.* Springer, 1984.

[29] L. Velho and D. Zorin. 4-8 subdivision. *Computer Aided Geometric Design*, 18:397–427, 2001.

[30] W. Welch and A. Witkin. Variational surface modeling. In *Computer Graphics (SIGGRAPH '92 Proceedings)*, pages 157–166, 1992.

[31] D. Zorin. Subdivision and multiresolution surface representations. *PhD thesis, Caltech, Pasadena*, 1997.

[32] D. Zorin. A method for analysis of C^1–continuity of subdivision surfaces. *SIAM Jour. of Numerical Analysis*, 37(4), 2000.

[33] D. Zorin, P. Schröder, and W. Sweldens. Interpolating subdivision for meshes with arbitrary topology. In *Computer Graphics (SIGGRAPH '96 Proceedings)*, pages 189–192, 1996.